Letter

Interplay of quantum resources in nonlocality tests

Hai-Hao Dong,[1,2,3] Yuwei Zhu,[4,5] Su-Yi Cheng,[1,2,3] Xingjian Zhang,[1,2,4] Cheng-Long Li,[1,2,3] Ying-Zhao Li,[1,2,3] Hao Li,[6] Lixing You,[6] Xiongfeng Ma,[3,4,*] Qiang Zhang,[1,2,3,†] and Jian-Wei Pan[1,2,3,‡]

[1]*Hefei National Research Center for Physical Sciences at the Microscale and School of Physical Sciences, University of Science and Technology of China, Hefei, China*

[2]*Shanghai Research Center for Quantum Science and CAS Center for Excellence in Quantum Information and Quantum Physics, University of Science and Technology of China, Shanghai, China*

[3]*Hefei National Laboratory, University of Science and Technology of China, Hefei, China*

[4]*Center for Quantum Information, Institute for Interdisciplinary Information Sciences, Tsinghua University, Beijing 100084, People's Republic of China*

[5]*Yau Mathematical Sciences Center, Tsinghua University, Beijing 100084, People's Republic of China*

[6]*Shanghai Key Laboratory of Superconductor Integrated Circuit Technology, Shanghai Institute of Microsystem and Information Technology, Chinese Academy of Sciences, Shanghai 200050, China*

(Received 9 September 2024; revised 15 January 2025; accepted 28 April 2025; published 5 June 2025)

Nonlocality, evidenced by the violation of Bell inequalities, not only signifies entanglement but also highlights measurement incompatibility in quantum systems. Utilizing the tilted Clauser-Horne-Shimony-Holt (CHSH) Bell inequality, our high-efficiency optical setup achieves a loophole-free violation of 2.0132. This result provides a device-independent lower bound on entanglement, quantified as the entanglement of formation at 0.0159. Moreover, by tuning the parameters of the tilted CHSH inequality, we enhance the estimation of measurement incompatibility, which is quantified by an effective overlap of 4.3883×10^{-5}. To explore the intricate interplay among nonlocality, entanglement, and measurement incompatibility, we generate mixed states, allowing for flexible modulation of entanglement via fast switching among the four Bell states using Pockels cells, achieving a fidelity above 99.10%. Intriguingly, our results reveal a counterintuitive relationship where increasing incompatibility initially boosts nonlocality but eventually leads to its reduction. Typically, maximal nonlocality does not coincide with maximal incompatibility. This experimental study sheds light on the optimal management of quantum resources for Bell-inequality-based quantum information processing.

DOI: 10.1103/PhysRevResearch.7.L022055

Introduction. In response to Einstein, Podolsky, and Rosen's argument that quantum physics is an "incomplete" theory based on the local realism assumption [1], Bell proved that the predictions of quantum theory are incompatible with those of any physical theory satisfying local hidden-variable (LHV) models. This incompatible difference involves three quantum resources: *Bell nonlocality*, *entanglement*, and *measurement incompatibility* [2]. Specifically, we speak of Bell nonlocality when LHV models do not hold [3], which is indicated by the violation of Bell inequalities [4]. Entanglement characterizes the nonclassical nature of a composite system state that cannot be decomposed into a product of individual subsystem states. Incompatibility goes back to Heisenberg's uncertainty principle [5], indicating the presence of quantum measurements that cannot be simultaneously implemented. While both entanglement and measurement incompatibility are necessary conditions for nonlocality, the study of the significance of measurement incompatibility in nonlocality tests has progressed slowly, leaving it a potential area of research [6–13]. In addition to their significance for testing quantum foundations, these three quantum resources have broad applications in quantum cryptography, including quantum key distribution [14–20] and quantum random number generation (QRNG) [21–28].

Given the essential role that a sufficient level of nonlocality, entanglement, and incompatibility plays in quantum protocols, quantifying these resources is fundamental and significant. Moreover, finding the quantitative relation among them is also important but remains unclear. Thanks to the necessity between entanglement, incompatibility, and nonlocality, nonlocality can provide valid estimations of these two resources, even in the presence of untrusted devices, known as *device-independent* (DI) quantification [15,17,29–37]. As for the interplay among the three, it is well established that only the maximal amount of entanglement and the maximal measurement incompatibility result in the highest CHSH nonlocality of $2\sqrt{2}$. Consequently, one might intuitively deduce that increasing entanglement or incompatibility leads

*Contact author: xma@tsinghua.edu.cn
†Contact author: qiangzh@ustc.edu.cn
‡Contact author: pan@ustc.edu.cn

to more nonlocality while keeping the other factor constant. However, the relationship among them can be counterintuitive. Theoretical studies have shown that when the amount of entanglement is fixed and considering all possible states, increasing the measurement incompatibility initially enhances nonlocality but eventually reduces it [38]. Additionally, other related works have revealed the counterintuitive phenomena among quantum resources in nonlocality tests [39–41].

In experiments, to observe the quantitative relationship, Bell violations in different combinations of entanglement and measurement incompatibility are needed. To make the results more general, these violations should be extended to a more general type of Bell inequality—tilted CHSH inequality. Achieving these outcomes convincingly, in a loophole-free manner [42–45], necessitates a spacelike separated system characterized by high detection efficiency and state fidelity. Additionally, a method for preparing mixed states with adjustable levels of entanglement is also required.

In this work, the experiments are first conducted in a device-independent manner by closing the locality and detection loopholes with the state-of-art efficiency in a spacelike separated Bell test setup. We considered the entanglement of formation (EOF) [29] as the entanglement measure because it can be quantitively estimated by a given Bell inequality violation. We also estimate the tight bound of measurement incompatibility defined by effective overlap [46].

To further investigate the interplay among nonlocality, entanglement, and incompatibility, we use a mixed-state preparation technique by fast switching between Bell bases with high frequency, efficiency, and fidelity. This approach allows the entanglement of the Bell diagonal states to be precisely controlled by electronic parameters.

Resources quantification via nonlocality test. For systematical investigation, we use a set of tilted CHSH-type Bell inequalities with an extra parameter α [39],

$$S_\alpha = \alpha\langle \hat{A}_0 \otimes \hat{B}_0\rangle + \alpha\langle \hat{A}_0 \otimes \hat{B}_1\rangle + \langle \hat{A}_1 \otimes \hat{B}_0\rangle - \langle \hat{A}_1 \otimes \hat{B}_1\rangle, \tag{1}$$

where $\langle \hat{A}_x \otimes \hat{B}_y\rangle = \sum_{a,b} ab \cdot p(a, b|x, y)$, $a, b \in \{\pm 1\}$. Here $p(a, b|x, y)$ denotes the outcome probability conditioned on the measurements $\hat{A}_x$ and $\hat{B}_y$ by Alice and Bob according to their measurement inputs, $x, y \in \{0, 1\}$, respectively. The parameter $\alpha \geqslant 1$ is an extra term partially tuning the contribution of inputs. When $\alpha = 1$, Eq. (4) reduces to the original CHSH value obtained in the game.

First, we use EOF as a measure of entanglement. Operationally, EOF provides a computable bound on the entanglement cost [29], which quantifies the optimal state conversion rate of diluting maximally entangled states into the desired states under local operations and classical communication. Theoretically,

$$E_{\mathrm{F}}(\rho_{AB}) \geqslant \frac{S_\alpha - 2\alpha}{2\sqrt{1+\alpha^2} - 2\alpha}, \tag{2}$$

where ρ_{AB} is the underlying state shared by Alice and Bob.

As for incompatibility, we use the effective overlap to measure it. This measure is state dependent and can be tested experimentally [46]. In the standard CHSH case, the quantity is effectively upper bounded by

$$c^*(\rho_A, A_0, A_1) \leqslant \frac{1}{2} + \frac{S}{8}\sqrt{8 - S^2}, \tag{3}$$

wherein the incompatibility is thus lower bounded by $\min\{c^*, 1 - c^*\}$. One can find more explanation about these measures and multi-α incompatibility estimation results in Supplemental Material Sec. I [47]. The experimental setup is shown in Fig. 1. The polarization-entangled 1560 nm photon pairs are created by spontaneous parameter down conversion (SPDC) in the Sagnac loop from a 780 nm pump laser with a pulse width of 10 ns and a repetition rate of 200 kHz. Then, the photon pairs are transmitted to Alice's and Bob's laboratories separately through fiber channels for independent measurements. To close the *locality loophole*, we separate Alice's and Bob's measurement stations far enough apart and apply fast measurements and precise synchronization. The synchronization of the experimental system is achieved by locking the pump laser, the QRNG for the setting choice, and the time-to-digital converter (TDC) for signal collection to the same clock (CLK), as shown in Fig. 1. We carefully adjust the relative delay between the QRNG and pump light to ensure that the polarization of the photons can be modulated when the setting choice signal is applied to the Pockels cell simultaneously. We designate the detection event on the transmission path of the PBS as $a(b) = 1$; otherwise, $a(b) = -1$ for each trial. The overall detection efficiencies are $82.8\% \pm 0.2\%$ for Alice and $82.7\% \pm 0.2\%$ for Bob, respectively, which are high enough to realize a CHSH violation without postselection and to close the *detection loophole*.

After 8 h, 5.76×10^9 trials of experiment, the final quantity S_α of interest, defined by Eq. (1), can be calculated from

$$\langle \hat{A}_x \otimes \hat{B}_y\rangle = \frac{N_{-1,-1|xy} - N_{-1,1|xy} - N_{1,-1|xy} + N_{1,1|xy}}{N_{xy}}, \tag{4}$$

where N_{xy} is the number of trials with inputs x and y. A trial is counted if and only if Alice and Bob both randomly choose a setting at which to perform a measurement. And $N_{ab|xy}$ is the number of correlated events with outputs a and b, given x and y. We set the coincidence window to be 15 ns and obtain eight distinct CHSH values S by varying the mean photon number per pulse. In Fig. 2(a), we quantify the entanglement of the underlying states of these eight results using EOF. For instance, upon reaching $S = 2.0132$, we certify the EOF in the underlying state to be 0.0159. More entanglement estimation results and the P values of CHSH violation S are provided in Supplemental Material Sec. III [47], where the P value can be defined as the maximum probability, according to local realism, of observing a violation at least as high as that achieved in the experiment [48].

Next, we obtain the quantification results for incompatibility using c^*. The estimation results are depicted in Fig. 2(b). Additionally, by varying the parameter α when $S = 2.0098$, we observe that, for specific $\alpha > 1$, a more precise estimation can be achieved via the CHSH-type expression given in Eq. (1). The estimation via multiple values of α is detailed in Supplemental Material Sec. I [47]. In Fig. 2(c), the optimal estimation of incompatibility, 1.12×10^{-4}, is achieved at $\alpha = 1.04$ among the provided options.

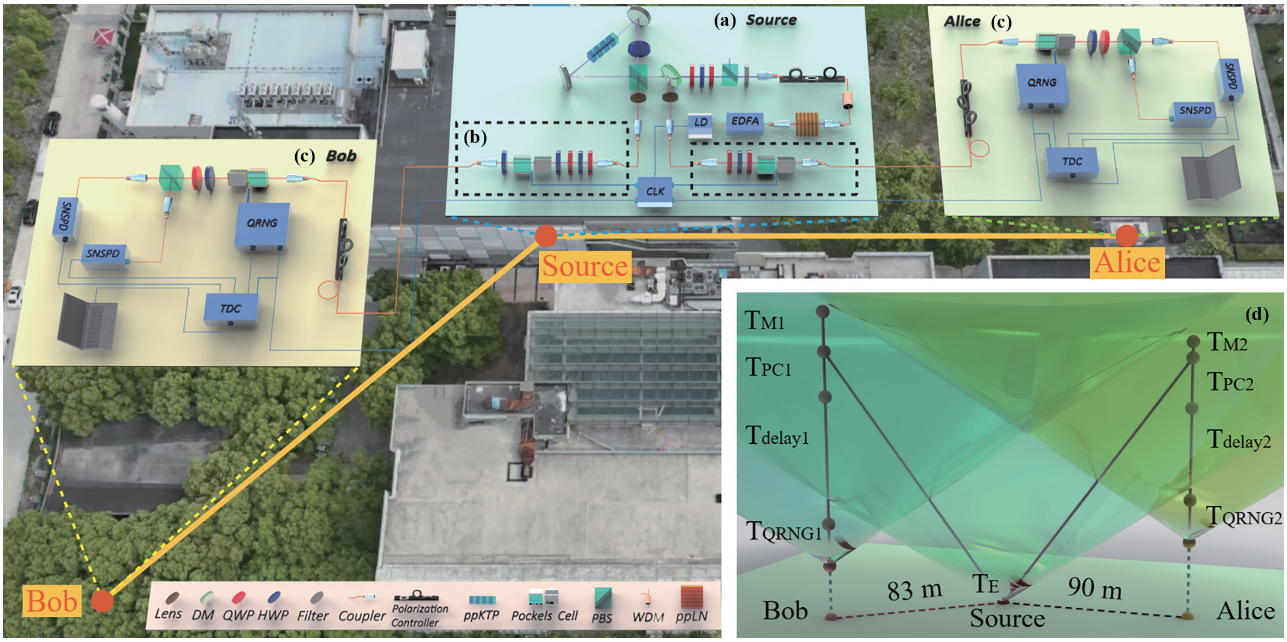

FIG. 1. Schematics of the experiment setup. (a) Preparation of entangled photon pairs. (b) Preparation of the Bell diagonal state in Eq. (5). (c) Single photon polarization state measurements for Alice and Bob, respectively, consist of a polarization controller (PC), a Pockels cell, a half-wave plate (HWP), a polarizing beam splitter (PBS), and finally a superconducting nanowire single-photon detector (SNSPD). For the DI entanglement and measurement incompatibility evaluation experiment, there is only one detector on the transmission port of the PBS; for the interplay experiment, there are two detectors on both the transmission and reflection ports for postselection. (d) The space-time correlation of the experiment. T_{E} is the time needed to create entangled photon pairs. $T_{\mathrm{QRNG1,2}}$ represents the duration for generating random bits to switch Pockels cells. $T_{\mathrm{delay1,2}}$ is the interval between random bit generation and delivery to the Pockels cells. $T_{\mathrm{PC1,2}}$ indicates the delay for Pockels cells to prepare for state measurements after receiving the random bits. $T_{\mathrm{M1,2}}$ denotes the duration for SNSPD to produce electronic signals. The details can be seen in Supplemental Material Sec. III [47].

Interplay among three quantum resources. In the previous part, by optimizing the entanglement, we obtain a monotonic relationship between nonlocality and incompatibility, as shown in Eq. (3). Here, we extend our previous findings by investigating a more general interplay among these three pivotal quantities in quantum physics.

In our experimental demonstration, we plot the curves representing the relationship between measurement incompatibility and nonlocality for various states with a fixed amount of entanglement. We then construct the convex hull of these curves to illustrate the overall relationship between measurement incompatibility and nonlocality for this given amount of entanglement. We maintain the fixed amount of entanglement in the Bell-diagonal state,

$$\rho_\lambda = \lambda_1|\Psi^+\rangle\langle\Psi^+| + \lambda_2|\Psi^-\rangle\langle\Psi^-| + \lambda_3|\Phi^+\rangle\langle\Phi^+| + \lambda_4|\Phi^-\rangle\langle\Phi^-|, \tag{5}$$

where $|\Phi^\pm\rangle = (|00\rangle \pm |11\rangle)/\sqrt{2}$, $|\Psi^\pm\rangle = (|01\rangle \pm |10\rangle)/\sqrt{2}$ are four Bell bases. The measurements we choose are parametrized as $\hat{A}_0 = \sigma_z, \hat{A}_1 = \sigma_x, \hat{B}_0 = \cos\theta\sigma_z + \sin\theta\sigma_x, \hat{B}_1 = \cos\theta\sigma_z - \sin\theta\sigma_x$, while the angular difference θ between two linear polarization measurements at Bob is varied to change the incompatibility (see Supplemental Material Sec. II [47] for details). In this case, θ is monotonically related to c^*, where $c^* = \cos^2\theta, \theta \in [0, \pi/4]$. When $\theta = 0$, $\hat{B}_0$ and $\hat{B}_1$ are totally compatible and, when $\theta = \pi/4$, they have the maximal incompatibility. To illustrate the interplay, we take concurrence and one-way distillable entanglement (ODE) as the target entanglement measures, since the former captures EOF and the latter captures entanglement entropy for the Bell-diagonal state, respectively. For a given level of concurrence, it has been established that the maximal tilted CHSH Bell value corresponds to a specific state [38]. In our experimental setup, we select the state that always attains the maximal nonlocality (tilted CHSH

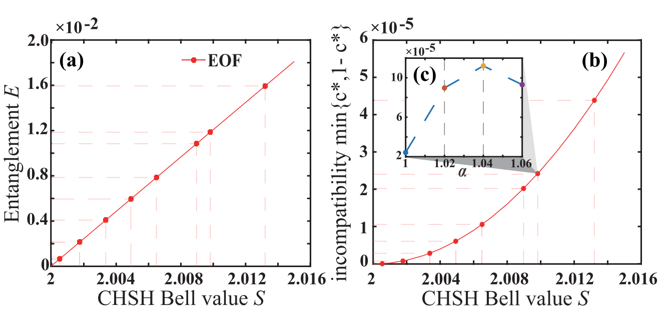

FIG. 2. (a) Diagram of EOF estimation results in the DI experiment. We plot the theoretical estimated results of EOF with a red solid line and mark the experimental estimated results of EOF with red dots on the line. (b) Diagram of incompatibility estimation results in the DI experiment. We plot the theoretical estimated results of $\min\{c^*, 1 - c^*\}$ with a red solid line and mark the experimental estimated results with red dots. (c) Subdiagram of (b), illustrating the incompatibility estimation results with discrete multiple α using the DI experiment statistics of $S = 2.0098$.

TABLE I. States for analysis of the interplay among entanglement, nonlocality, and measurement incompatibility.

	$C = 0.4$	$E_D^{\rightarrow} = 0.2$			$E_D^{\rightarrow} = 0.1$		
	State 0	State 1	State 2	State 3	State 4	State 5	State 6
λ_1	0.7	0.788	0.832	0.847	0.797	0.765	0.712
λ_2	0.3	0.203	0.132	0.079	0.163	0.215	0.284
λ_3	0	0.006	0.031	0.068	0.033	0.016	0.003
λ_4	0	0.002	0.005	0.006	0.007	0.004	0.001

violation) for concurrence $C = 0.4$. For the ODE, we select three states each for $E_D^{\rightarrow} = 0.1$ and $E_D^{\rightarrow} = 0.2$, respectively, in order to plot their convex hull. And we analyze the α-CHSH value for $\alpha = 1$ and $\alpha = 1.5$ separately. The specific states chosen for this analysis are detailed in Table I.

The preparation of the four Bell states is achieved using an entanglement source, along with two sets of wave plates and Pockels cells. The Bell state $|\Psi^+\rangle$ is directly generated from the source. The other three Bell states can be obtained by transforming $|\Psi^+\rangle$ through the following operations:

$$
\begin{aligned}
|\Psi^-\rangle &= \sigma_z \otimes I \cdot |\Psi^+\rangle, \\
|\Phi^+\rangle &= I \otimes \sigma_x \cdot |\Psi^+\rangle, \\
|\Phi^-\rangle &= \sigma_z \otimes \sigma_x \cdot |\Psi^+\rangle,
\end{aligned} \tag{6}
$$

where σ_x, σ_y, and σ_z are the Pauli operators. In our experimental setup, as shown in Fig. 1(b), when a high voltage is applied to the Pockels cell, the σ_z (σ_x) operation is performed along the path to Alice's (Bob's) side with the help of wave plates; otherwise, the identity operation I is applied. According to the parameters $\{\lambda_1, \lambda_2, \lambda_3, \lambda_4\}$ in Table I, we allocate the proportions of the four Bell states within a 5 ms cycle. After a long accumulation period (in our experiment, each Bell diagonal state is accumulated for 100 minutes), the target state can be statistically obtained, with a fidelity exceeding 99.10%. At the measurement stations, we keep Alice's measurement settings constant while changing Bob's measurement settings every ten minutes. We rotate Bob's HWP from 22.5° to 11.25° in 100 min with a step of −1.25° to change the difference θ between Bob's two measurements, which corresponds to the measurement incompatibility. See Supplemental Material Sec. III [47] for details.

Finally, we apply postselection to process the acquired data. Due to the use of SPDC sources, the photon count follows a Poisson distribution [49], resulting in a significant number of vacuum states. In the absence of postselection, this leads to a mixture of the target state, as shown in Table I, and vacuum states, causing deviations in the amount of entanglement from the designed value. To filter out the vacuum events, we utilize two SNSPDs at each measurement station.

By varying the level of incompatibility using $\theta \in [0, \pi/4]$ in 10 points, we observe the curves of states with $C = 0.4$ ($E_D^{\rightarrow} = 0.2$) using the original CHSH inequality and the tilted CHSH inequality in Figs. 3(a) and 3(b) [3(c) and 3(d)], respectively. To illustrate the results, we use Fig. 3(d) as an example. We depict the curves of states 1, 2, and 3, all of which have $E_D^{\rightarrow} = 0.2$. The resulting interplay curve is represented by the convex hull of these three curves, shown by the dark solid line. This experiment clearly shows the interplay among the three quantum resources.

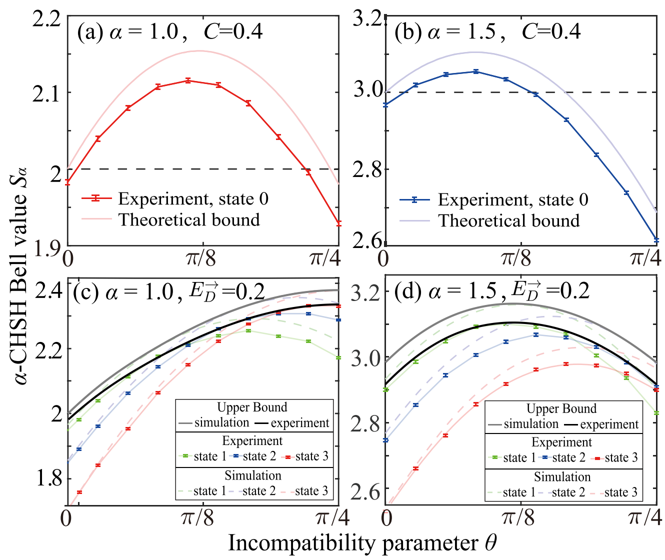

FIG. 3. Interplay between nonlocality and incompatibility under a fixed amount of entanglement. In panels (a) and (b), the maximal α-CHSH values from the experiment with $C = 0.4$ are presented. The red and blue line segments (with error bars) illustrate the interplay between nonlocality and incompatibility. The faint solid line represents the theoretical upper bound. In panels (c) and (d), the curves of states 1, 2, and 3 (all with $E_D^{\rightarrow} = 0.2$) are shown as faint line segments with error bars. The resulting convex-hull interplay curves are represented by dark solid lines and the theoretical curve is shown as dashed lines and faint gray lines.

In Fig. 3(c), we observe that maximal CHSH nonlocality is achieved at maximal incompatibility. In contrast, in 3(a), 3(b), and 3(d), we see an unexpected phenomenon: increasing incompatibility initially raises the value of the α-CHSH inequality, but eventually causes it to decrease. Our experimental findings reveal a counterintuitive correlation: while entanglement remains constant, maximal nonlocality is typically not attained at the highest level of measurement incompatibility. This highlights the generic interplay among nonlocality, entanglement, and incompatibility. Additionally, our experimental curves align perfectly with our theoretical simulation curves, confirming the robustness of our theoretical results [47].

Conclusion and discussion. In conclusion, we have demonstrated a device-independent method to quantify the entanglement and measurement incompatibility of a quantum system. By successfully closing various loopholes in the optical system, we show that a loophole-free Bell test setup can quantify a significant amount of entanglement based on EOF. Also, we optimize the estimation of measurement incompatibility by changing the parameter α of the tilted CHSH inequality.

With the quantification of entanglement through nonlocality, we delve into the interplay among nonlocality, entanglement, and measurement incompatibility. Our experimental findings reveal a counterintuitive phenomenon within quantum mechanics: given a fixed amount of entanglement and considering all possible states, an increase in measurement incompatibility unexpectedly leads to a reduction in the achievable Bell nonlocality. This runs counter to the conventional expectation that greater quantum resources should necessarily enhance violations of locality. Specifically, the emergence or absence of this counterintuitive interplay depends on the choice of entanglement measures (e.g., concurrence versus ODE) and the use of tilted-CHSH inequalities ($\alpha = 1$ versus $\alpha > 1$). This surprising observation challenges established notions and underscores the intricate subtleties of quantum theory.

Building upon this discovery, we present that, given a certain amount of entanglement, two distinct levels of incompatibility can yield equivalent nonlocality. Our results inspire several potential research directions, including the optimization of states and measurement resources in Bell-inequality-based quantum information processing protocols, such as device-independent QRNG and device-independent quantum key distribution.

Acknowledgments. This work has been supported by the National Natural Science Foundation of China (Grants No. T2125010 and No. 12174216), the Shanghai Municipal Science and Technology Major Project (Grant No. 2019SHZDZX01), the Anhui Initiative in Quantum Information Technologies (Grant No. AHY010300), and the Innovation Program for Quantum Science and Technology (Grants No. 2021ZD0300800, No. 2023ZD0300100, No. 2021ZD0300804 and No. 2021ZD0300702).

H.-H.D., Y.Z., and S.-Y.C. contibuted equally to this work.

Data Availability. The data that support the findings of this Letter are not publicly available. The data are available from the authors upon reasonable request.

[1] A. Einstein, B. Podolsky, and N. Rosen, Can quantum-mechanical description of physical reality be considered complete? Phys. Rev. **47**, 777 (1935).

[2] E. Chitambar and G. Gour, Quantum resource theories, Rev. Mod. Phys. **91**, 025001 (2019).

[3] V. Scarani, *Bell Nonlocality* (Oxford University Press, Oxford, 2019).

[4] N. Brunner, D. Cavalcanti, S. Pironio, V. Scarani, and S. Wehner, Bell nonlocality, Rev. Mod. Phys. **86**, 419 (2014).

[5] W. Heisenberg, Über den anschaulichen inhalt der quantentheoretischen kinematik und mechanik, Z. Phys. **43**, 172 (1927).

[6] S. Designolle, P. Skrzypczyk, F. Fröwis, and N. Brunner, Quantifying measurement incompatibility of mutually unbiased bases, Phys. Rev. Lett. **122**, 050402 (2019).

[7] S.-L. Chen, N. Miklin, C. Budroni, and Y.-N. Chen, Device-independent quantification of measurement incompatibility, Phys. Rev. Res. **3**, 023143 (2021).

[8] D. Cavalcanti and P. Skrzypczyk, Quantitative relations between measurement incompatibility, quantum steering, and nonlocality, Phys. Rev. A **93**, 052112 (2016).

[9] R. Uola, T. Kraft, S. Designolle, N. Miklin, A. Tavakoli, J.-P. Pellonpää, O. Gühne, and N. Brunner, Quantum measurement incompatibility in subspaces, Phys. Rev. A **103**, 022203 (2021).

[10] E. Bene and T. Vértesi, Measurement incompatibility does not give rise to bell violation in general, New J. Phys. **20**, 013021 (2018).

[11] S. Egelhaaf, J. Pauwels, M. T. Quintino, and R. Uola, Certifying measurement incompatibility in prepare-and-measure and bell scenarios, J. Phys. A **58**, 095304 (2025).

[12] F. Hirsch, M. T. Quintino, and N. Brunner, Quantum measurement incompatibility does not imply bell nonlocality, Phys. Rev. A **97**, 012129 (2018).

[13] S. Designolle, M. Farkas, and J. Kaniewski, Incompatibility robustness of quantum measurements: a unified framework, New J. Phys. **21**, 113053 (2019).

[14] A. K. Ekert, Quantum cryptography based on Bell's theorem, Phys. Rev. Lett. **67**, 661 (1991).

[15] D. Mayers and A. Yao, Quantum cryptography with imperfect apparatus, in *Proceedings of the 39th Annual Symposium on Foundations of Computer Science (Cat. No.98CB36280)* (IEEE, Palo Alto, CA, 1998), pp. 503–509.

[16] J. Barrett, L. Hardy, and A. Kent, No signaling and quantum key distribution, Phys. Rev. Lett. **95**, 010503 (2005).

[17] A. Acín, N. Brunner, N. Gisin, S. Massar, S. Pironio, and V. Scarani, Device-independent security of quantum cryptography against collective attacks, Phys. Rev. Lett. **98**, 230501 (2007).

[18] W.-Z. Liu, Y.-Z. Zhang, Y.-Z. Zhen, M.-H. Li, Y. Liu, J. Fan, F. Xu, Q. Zhang, and J.-W. Pan, Toward a photonic demonstration of device-independent quantum key distribution, Phys. Rev. Lett. **129**, 050502 (2022).

[19] D. P. Nadlinger, P. Drmota, B. C. Nichol, G. Araneda, D. Main, R. Srinivas, D. M. Lucas, C. J. Ballance, K. Ivanov, E.-Z. Tan *et al.*, Experimental quantum key distribution certified by Bell's theorem, Nature (London) **607**, 682 (2022).

[20] W. Zhang, T. van Leent, K. Redeker, R. Garthoff, R. Schwonnek, F. Fertig, S. Eppelt, W. Rosenfeld, V. Scarani, C. C.-W. Lim *et al.*, A device-independent quantum key distribution system for distant users, Nature (London) **607**, 687 (2022).

[21] S. Pironio, A. Acín, S. Massar, A. B. de La Giroday, D. N. Matsukevich, P. Maunz, S. Olmschenk, D. Hayes, L. Luo, T. A. Manning *et al.*, Random numbers certified by Bell's theorem, Nature (London) **464**, 1021 (2010).

[22] R. Colbeck and A. Kent, Private randomness expansion with untrusted devices, J. Phys. A: Math. Theor. **44**, 095305 (2011).

[23] P. Bierhorst, E. Knill, S. Glancy, Y. Zhang, A. Mink, S. Jordan, A. Rommal, Y.-K. Liu, B. Christensen, S. W. Nam *et al.*, Experimentally generated randomness certified by the impossibility of superluminal signals, Nature (London) **556**, 223 (2018).

[24] Y. Liu, Q. Zhao, M.-H. Li, J.-Y. Guan, Y. Zhang, B. Bai, W. Zhang, W.-Z. Liu, C. Wu, X. Yuan *et al.*, Device-independent quantum random-number generation, Nature (London) **562**, 548 (2018).

[25] Y. Zhang, L. K. Shalm, J. C. Bienfang, M. J. Stevens, M. D. Mazurek, S. W. Nam, C. Abellán, W. Amaya, M. W. Mitchell, H. Fu, C. A. Miller, A. Mink, and E. Knill, Experimental low-latency device-independent quantum randomness, Phys. Rev. Lett. **124**, 010505 (2020).

[26] M.-H. Li, X. Zhang, W.-Z. Liu, S.-R. Zhao, B. Bai, Y. Liu, Q. Zhao, Y. Peng, J. Zhang, Y. Zhang *et al.*, Experimental realization of device-independent quantum randomness expansion, Phys. Rev. Lett. **126**, 050503 (2021).

[27] L. K. Shalm, Y. Zhang, J. C. Bienfang, C. Schlager, M. J. Stevens, M. D. Mazurek, C. Abellán, W. Amaya, M. W. Mitchell, M. A. Alhejji *et al.*, Device-independent randomness expansion with entangled photons, Nat. Phys. **17**, 452 (2021).

[28] C.-L. Li, K.-Y. Zhang, X. Zhang, K.-X. Yang, Y. Han, S.-Y. Cheng, H. Cui, W.-Z. Liu, M.-H. Li, Y. Liu *et al.*, Device-independent quantum randomness–enhanced zero-knowledge proof, Proc. Natl. Acad. Sci. USA **120**, e2205463120 (2023).

[29] C. H. Bennett, D. P. DiVincenzo, J. A. Smolin, and W. K. Wootters, Mixed-state entanglement and quantum error correction, Phys. Rev. A **54**, 3824 (1996).

[30] V. Vedral, M. B. Plenio, M. A. Rippin, and P. L. Knight, Quantifying entanglement, Phys. Rev. Lett. **78**, 2275 (1997).

[31] F. Verstraete and M. M. Wolf, Entanglement versus Bell violations and their behavior under local filtering operations, Phys. Rev. Lett. **89**, 170401 (2002).

[32] Y.-C. Liang, T. Vértesi, and N. Brunner, Semi-device-independent bounds on entanglement, Phys. Rev. A **83**, 022108 (2011).

[33] T. Moroder, J.-D. Bancal, Y.-C. Liang, M. Hofmann, and O. Gühne, Device-independent entanglement quantification and related applications, Phys. Rev. Lett. **111**, 030501 (2013).

[34] G. Tóth, T. Moroder, and O. Gühne, Evaluating convex roof entanglement measures, Phys. Rev. Lett. **114**, 160501 (2015).

[35] R. Arnon-Friedman and H. Yuen, Noise-tolerant testing of high entanglement of formation, in *45th International Colloquium on Automata, Languages, and Programming (ICALP 2018)*, Leibniz International Proceedings in Informatics (LIPIcs), edited by I. Chatzigiannakis, C. Kaklamanis, D. Marx, and D. Sannella (Schloss Dagstuhl – Leibniz-Zentrum für Informatik, Dagstuhl, Germany, 2018), Vol. 107, pp. 11:1–11:12.

[36] S.-L. Chen, C. Budroni, Y.-C. Liang, and Y.-N. Chen, Exploring the framework of assemblage moment matrices and its applications in device-independent characterizations, Phys. Rev. A **98**, 042127 (2018).

[37] R. Arnon-Friedman and J.-D. Bancal, Device-independent certification of one-shot distillable entanglement, New J. Phys. **21**, 033010 (2019).

[38] Y. Zhu, X. Zhang, and X. Ma, Interplay among entanglement, measurement incompatibility, and nonlocality, Quantum Sci. Technol. **9**, 045008 (2024).

[39] A. Acín, S. Massar, and S. Pironio, Randomness versus nonlocality and entanglement, Phys. Rev. Lett. **108**, 100402 (2012).

[40] L. Wooltorton, P. Brown, and R. Colbeck, Device-independent quantum key distribution with arbitrarily small nonlocality, Phys. Rev. Lett. **132**, 210802 (2024).

[41] L. Tendick, H. Kampermann, and D. Bruß, Quantifying necessary quantum resources for nonlocality, Phys. Rev. Res. **4**, L012002 (2022).

[42] B. Hensen, H. Bernien, A. E. Dréau, A. Reiserer, N. Kalb, M. S. Blok, J. Ruitenberg, R. F. Vermeulen, R. N. Schouten, C. Abellán *et al.*, Loophole-free Bell inequality violation using electron spins separated by 1.3 kilometres, Nature (London) **526**, 682 (2015).

[43] L. K. Shalm, E. Meyer-Scott, B. G. Christensen, P. Bierhorst, M. A. Wayne, M. J. Stevens, T. Gerrits, S. Glancy, D. R. Hamel, M. S. Allman *et al.*, Strong loophole-free test of local realism, Phys. Rev. Lett. **115**, 250402 (2015).

[44] M. Giustina, M. A. M. Versteegh, S. Wengerowsky, J. Handsteiner, A. Hochrainer, K. Phelan, F. Steinlechner, J. Kofler, J.-A. Larsson, C. Abellán *et al.*, Significant-loophole-free test of Bell's theorem with entangled photons, Phys. Rev. Lett. **115**, 250401 (2015).

[45] M.-H. Li, C. Wu, Y. Zhang, W.-Z. Liu, B. Bai, Y. Liu, W. Zhang, Q. Zhao, H. Li, Z. Wang *et al.*, Test of local realism into the past without detection and locality loopholes, Phys. Rev. Lett. **121**, 080404 (2018).

[46] M. Tomamichel and E. Hänggi, The link between entropic uncertainty and nonlocality, J. Phys. A: Math. Theor. **46**, 055301 (2013).

[47] See Supplemental Material at http://link.aps.org/supplemental/10.1103/PhysRevResearch.7.L022055 for additional information about the experimental methods and theoretical simulations.

[48] Y. Zhang, S. Glancy, and E. Knill, Asymptotically optimal data analysis for rejecting local realism, Phys. Rev. A **84**, 062118 (2011).

[49] V. Caprara Vivoli, P. Sekatski, J.-D. Bancal, C. C. W. Lim, B. G. Christensen, A. Martin, R. T. Thew, H. Zbinden, N. Gisin, and N. Sangouard, Challenging preconceptions about bell tests with photon pairs, Phys. Rev. A **91**, 012107 (2015).